Two-phase flow in porous media: Crossover from capillary fingering to compact invasion for drainage

M. Ferer,* Grant S. Bromhal, and Duane H. Smith
US DOE, National Energy Technology Laboratory, Morgantown, West Virginia 26507-0880, USA
(Received 20 April 2004; revised manuscript received 24 August 2004; published 8 February 2005)

It had been predicted that the capillary fingering observed at small capillary numbers should change or cross over to compact invasion at larger capillary numbers or longer times [D. Wilkinson, Phys. Rev. A **34**, 1380 (1986)]. We present results from pore-level modeling in two dimensions for the average position (related to the position of the interface) of the injected fluid as well as the width of the interface between the injected, nonwetting fluid and the defending, wetting fluid. These results are entirely consistent with the predicted crossover from the fractal flow characterized by invasion percolation with trapping (IPWT) to compact/linear/stable flow, where the position of the injected fluid advances linearly with time and where the width of the interface is constant. Furthermore, our results for the characteristic time, at which the crossover occurs, agree with the predictions of Wilkinson. To focus on the effect of capillary number, we are considering only viscosity-matched flows where both fluids have the same viscosities. To our knowledge, these are the first pore-level modeling results that quantitatively test the general predictions of Wilkinson for this capillary crossover in the case of drainage. Our modeling results are used to provide closed form expressions predicting the dependence of average position and interfacial width upon capillary number and time, regardless of the size of the system. The size scaling inherent in the crossover combined with our results locating the upper and lower bounds of the crossover regime enable us to predict the location of the crossover for two-dimensional systems of different size. These predictions are compared with flow patterns from experiments in the literature. The agreement between our predictions and the experimental flow patterns indicates that the experiments exhibit the same IPWT to compact crossover observed in our modeling.

DOI: 10.1103/PhysRevE.71.026303 PACS number(s): 47.55.Mh, 47.53.+n, 47.20.Ma, 82.20.Wt

I. INTRODUCTION

Flow through porous media is a subject of scientific and engineering interest because of applications to enhanced oil recovery, dense nonaqueous phase liquid (DNAPL) remediation, and geologic CO_2 sequestration, to name a few. For half a century, flow in porous media has been treated as a compact (i.e., Euclidean) process whereby the interface advances linearly with the total amount of injected fluid. However, it had been predicted that the fractal capillary fingering observed at small capillary numbers should only change or cross over to the expected compact invasion at larger capillary numbers or longer times [1]. The previously assumed compact behavior is predicted by a Darcy's law treatment, which uses saturation-dependent relative permeabilities, such as those of Buckley-Leverett or Koval [2–6]. For the past two decades, it has been appreciated that flow in porous media is fractal in certain well-defined limits [7–16].

In the limit of zero capillary number, where the injection velocity is infinitesimal, $V=0$ (i.e., quasistatic injection), the flow is known to be modeled by self-similar, invasion percolation fractals [16–18]. The definition of the capillary number is

$$N_c = \mu V/\sigma \cos\theta, \tag{1}$$

i.e., the ratio of the viscous drag forces (viscosity of the fluid times average fluid velocity, μV) to the capillary forces (proportional to interfacial tension, σ, and cosine of the contact angle θ). The invasion percolation model has been widely investigated both to determine its fundamental properties and to determine its predictions for practical problems [1,9,16–24].

We have developed a computer code which includes capillary and viscous forces allowing a study of drainage, where a nonwetting fluid is injected into the porous medium and displaces a wetting fluid [25,26]. Our model consists of spherical pores at the sites of a diamond lattice; these pores are connected by cylindrical throats of randomly chosen cross-sectional area. The model relates the flow velocity through a throat to the pressure drop across the throat modified by any capillary pressure. Conserving volume of our incompressible fluids, a modified Gauss-Seidel iteration is performed to find the pressure field and the resulting flow velocities. The fluids are then advanced in the porous medium using flow rules that we have tried to make as nonrestrictive as possible. This model is a generic pore-level model of the type that has been widely used for the past two decades [7–9,12–15,18,21,22,27–35]. Although our model has many features in common with these other pore-level models in the literature, there are specific differences which we have fully detailed in earlier references [25,26].

At sufficiently low capillary numbers, we have demonstrated that our model correctly reproduces the zero-capillary number results from invasion percolation with trapping (IPWT) [25]. Having validated our model in the limit of small capillary number, where the flow exhibits fractal fingering, we then studied the effect of increased capillary num-

*Permanent address: Department of Physics, West Virginia University, P.O. Box 6315, Morgantown, WV 26506-6315, USA.

ber on the flow, when the fluids had matched viscosities, i.e., both fluids had the same viscosity. For this case, Wilkinson predicted a fractal-to-compact crossover on a characteristic length scale:

$$\Lambda \propto N_c^{-\nu/(t+1-\beta+\nu)}. \quad (2)$$

For percolation in two dimensions, this exponent has the value $\nu/(t+1-\beta+\nu)=0.38$ [1,36]. This crossover is similar to one we had observed for miscible flows, where the flows crossed over from a DLA fractal to compact behavior as viscosity ratio was increased [12–15]. In a recent paper, our modeling results observed the crossover predicted by Wilkinson [1,26]. In the current paper, we present results (i) for the full crossover regime now including where the flow has become compact; (ii) for the interfacial width exhibiting the same IPWT to compact crossover as it crosses over from fractal growth to a stable saturated value; (iii) for a quantitative analysis of our data for the average position and the interfacial width showing good agreement with the predictions of Wilkinson [1,36]; and (iv) for a reinterpretation of experimental flow patterns and data from the literature providing experimental support for the observed crossover [36,37].

Although Wilkinson predicted such a crossover almost twenty years ago, to our knowledge, our work is the first quantitative observation of his general predictions [1,36,37].

II. CROSSOVER FROM CAPILLARY FINGERING TO COMPACT BUCKLEY LEVERETT FLOW

In this section, we study the flow as it deviates from IPWT with increasing capillary number [Eq. (2)] due to increased flow rate. Figure 1 compares the near-breakthrough flow patterns for IPWT [Fig. 1(a)] with near-breakthrough patterns for the model for three capillary numbers. For the smallest capillary number, $N_c=2.6\times10^{-6}$, one sees slight additions to the IPWT pattern. For the next capillary number, the pattern deviates more strongly from IPWT, becoming more compact.

Our investigation also determined the first and second moments, $\langle x\rangle$ and $\langle x^2\rangle$, of the saturation profile, allowing a determination of both the interfacial width, w, where $w^2=2(3\langle x^2\rangle-4\langle x\rangle^2+\langle x\rangle$ [39] and the average position, $\langle x\rangle$, of the injected fluid as a function of injected volume, V, or mass, m, or time. Since our program maintains a constant volume flow, q, to within a fraction of a percent, the volume is directly proportional to the time, $V=qt$, as is the mass of our incompressible fluids. An additional advantage of determining the temporal behavior of these length scales is their simple relationship to fractal dimension for fractal flows like those from IPWT. Since the mass of a fractal, m, is related to the linear dimension, $\langle x\rangle$ or $\langle w\rangle$, $t\propto m=A\langle x\rangle^{D_f-1}$, $\langle x(t)\rangle$ [also true for $\langle w(t)\rangle$ [38]] is given by

$$\langle x(t)\rangle = Bt^{1/(D_f-1)} = Bt^{1+\varepsilon}, \quad (3a)$$

$$\langle w(t)\rangle = Ct^{1/(D_f-1)} = Ct^{1+\varepsilon}, \quad (3b)$$

which defines the exponent, ε. Careful analysis from very large (250 million pores) systems has shown that the correct

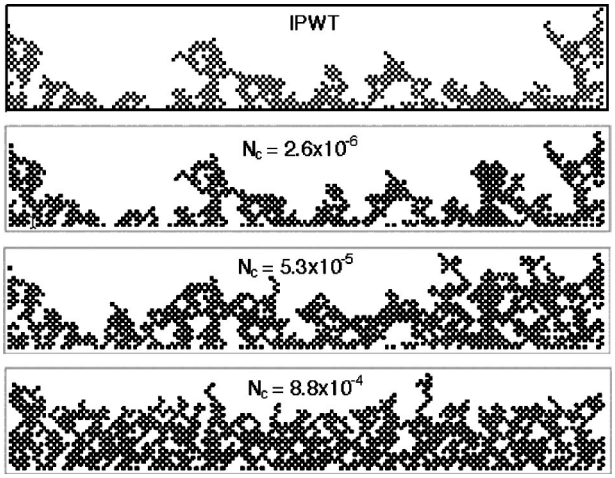

FIG. 1. Comparison of the near-breakthrough IPWT flow pattern (top) with the near-breakthrough patterns of our viscosity-matched fluids for three capillary numbers ($N_c=2.6\times10^{-6}$, $N_c=5.3\times10^{-5}$, and $N_c=8.8\times10^{-4}$) using one of the same realizations of the smallest model porous medium (30×90) studied in this paper. For the smallest of the three capillary numbers, the pattern is almost identical to that for IPWT. For the next capillary number, some of the IPWT flow pattern is still apparent although more of the porous medium has been invaded. For the largest of the two capillary numbers, the pattern is very different from the IPWT pattern with much more of the medium being invaded. In our modeling, we use short-wide ($L<W$) porous media because they represent the fingering more faithfully; the nonwetting fluid is injected into these short-wide media along the width (of size W) [26,38].

(i.e., limiting) value of the fractal dimension for IPWT is $D_f\approx1.825\pm0.005$ so that $\varepsilon\approx0.21$ [40]. However, for our small porous media systems, previous analysis of invasion percolation with trapping has indicated that $D_f\approx1.89$ so that $\varepsilon\approx0.13$ so that these "small-system" values are the ones that will be used in our analysis [25,26]. In order to compare modeling data for different flow rates and different widths, we define a time which is solely determined by the mass, m (or volume) per unit width, W, of injected fluid,

$$t \approx 0.91 + m/W, \quad (4)$$

where the constant 0.91 can simply be regarded as a fitting constant which only serves to reduce the deviations in early-time data from the dependence given in Eqs. (3). In an earlier paper, we argued that it could result from differences between discontinuous and discrete (our model) porous media [41]. Note that this definition of time allows a better comparison of systems with different flow velocities and widths but the same capillary number, because this time is related to real-time, t_R, by the q/W factor in capillary number, i.e., $t=0.91+qt_R/W$.

To best characterize any deviations from IPWT for each of the realizations, we determined the ratio $x_{N_c}(t)/x_{\mathrm{IP}}(t)$ until there were significant, sustained deviations from unity; from that point on, we used the ratio $x_{N_c}(t)/x_{\mathrm{IP,ave}}(t)$, where $x_{\mathrm{IP,ave}}(t)=0.445t^{1.13}$ for IPWT. For a range of capillary numbers, the values of these ratios were averaged over the five or more realizations of 30×90 and 30×135 systems (i.e., L

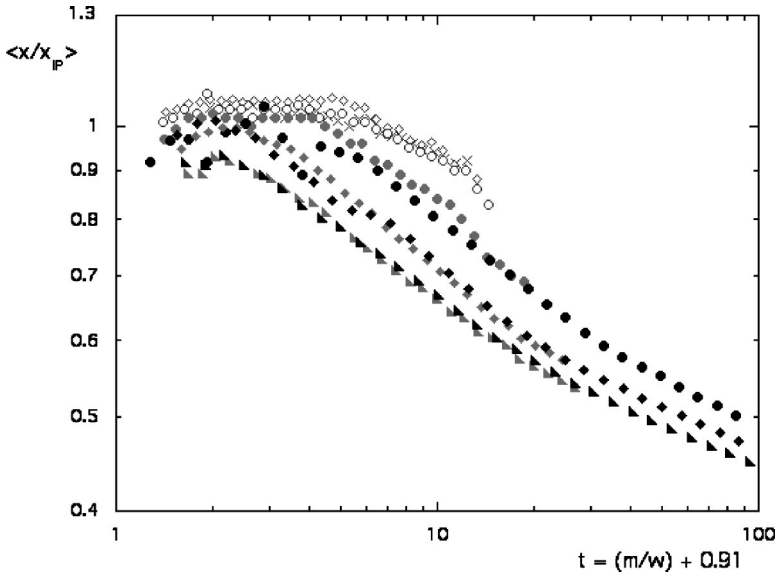

FIG. 2. The average position of the injected fluid for two system sizes and a variety of capillary numbers [$N_c=1.33\times10^{-5}$ (×) for $L=30$; $N_c=2.66\times10^{-5}$ (◇) for $L=30$; $N_c=5.31\times10^{-5}$ (○) for $L=30$; $N_c=2.12\times10^{-4}$ (●) for $L=30$ and (●) for $L=90$; $N_c=8.85\times10^{-4}$ (◆) for $L=30$ and (◆) for $L=90$; and $N_c=3.54\times10^{-3}$ (▶) for $L=30$ and (▶) for $L=90$]. Initially, the flow is IPWT-like, $x\approx x_{\mathrm{IP}}$; but then the flow begins to become compact at a characteristic time which varies inversely with capillary number. The plot only presents every third point to enhance the clarity of the legend. Differences between the $L=30$ results (gray scale) and the $L=90$ results provide an estimate of the errors in the data.

$=30$ in the direction of flow) and, separately, averaged over several realizations of 90×90 and 90×180 (i.e., $L=90$) systems. These results are shown in Fig. 2. At small times and small capillary numbers, the results are characteristic of IPWT fractals, i.e., $x/x_{\mathrm{IP}}\approx1$, but then they break away from the IPWT behavior at a characteristic time which varies inversely with capillary number. It should be noted that breakthrough occurs for times, $t\approx20$, in the $L=30$ systems, but that it occurs for $t\approx100$ in the $L=90$ systems.

The interfacial width exhibits similar behavior, in mimicking the IPWT behavior $w_{\mathrm{IP}}\approx t^{1/(D_f-1)}$ for small times and capillary numbers [38], but then breaking away at the characteristic time. Unfortunately, the long-time width in the larger systems is noisier than is the average position. This may be due to marginal stability of the interface for our small systems.

Wilkinson predicted that, in two dimensions, the characteristic crossover length should scale as the 0.381 power of capillary number; therefore, the characteristic time should scale as the $0.381(D_f-1)\approx0.31$ power of capillary number,

$$\tau(N_c)\approx N_c^{-0.31}. \tag{5}$$

If this is the correct form for the characteristic time, a plot of the length scales, $\langle x\rangle$ or $\langle w\rangle$ in Figs. 2 and 3 should collapse to one "universal" curve when plotted vs t/τ,

$$\langle x(t)\rangle = 0.445t^{1.13}\chi(t/\tau). \tag{6a}$$

$$\langle w(t)\rangle = 0.53t^{1.13}\Omega(t/\tau). \tag{6b}$$

For both length scales, Wilkinson's predicted characteristic time, Eq. (5), does collapse the data to a universal curve so that Eqs. (6) correctly include all of the capillary number dependence of the two phase flow. It should be noted that Wilkinson used general flow and percolation theory arguments, which were independent of a particular porous media structure, in both two and three dimensions. Therefore, if his results are valid for our simplistic, diamond-lattice porous media structure, this is evidence that they should be valid in general for any standard porous media structure in two dimensions. Further, this is evidence that the derivation is valid

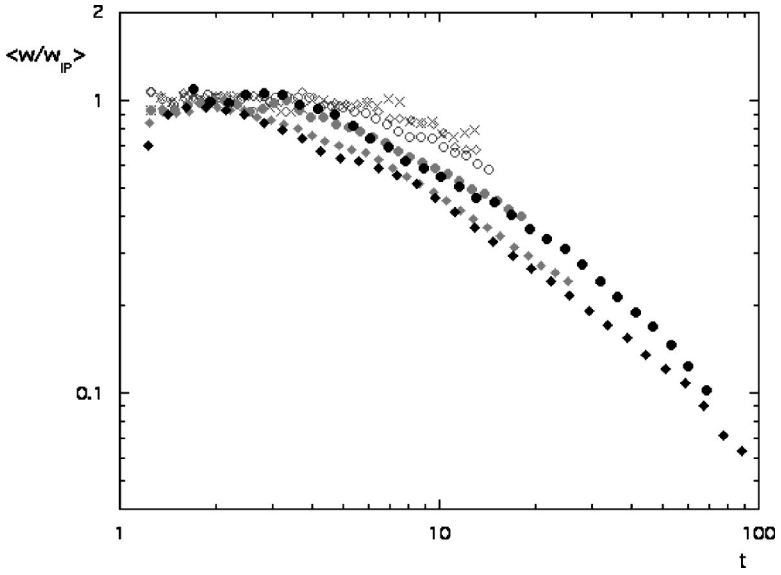

FIG. 3. The average interfacial width for two system sizes and a variety of capillary numbers [$N_c=1.33\times10^{-5}$ (×) for $L=30$; $N_c=2.66\times10^{-5}$ (◇) for $L=30$; $N_c=5.31\times10^{-5}$ (○) for $L=30$; $N_c=2.12\times10^{-4}$ (●) for $L=30$ and (●) for $L=90$; and $N_c=8.85\times10^{-4}$ (◆) for $L=30$ and (◆) for $L=90$]. Initially, the flow is IPWT-like, $w\approx w_{\mathrm{IP}}$; but then the flow begins to cross over to stable behavior at a characteristic time which varies inversely with capillary number as did the average position in Fig. 2. As in Fig. 2, the plot only presents every third point to enhance the clarity of the legend, and differences between the $L=30$ results (gray scale) and the $L=90$ results provide an estimate of the errors in the data.

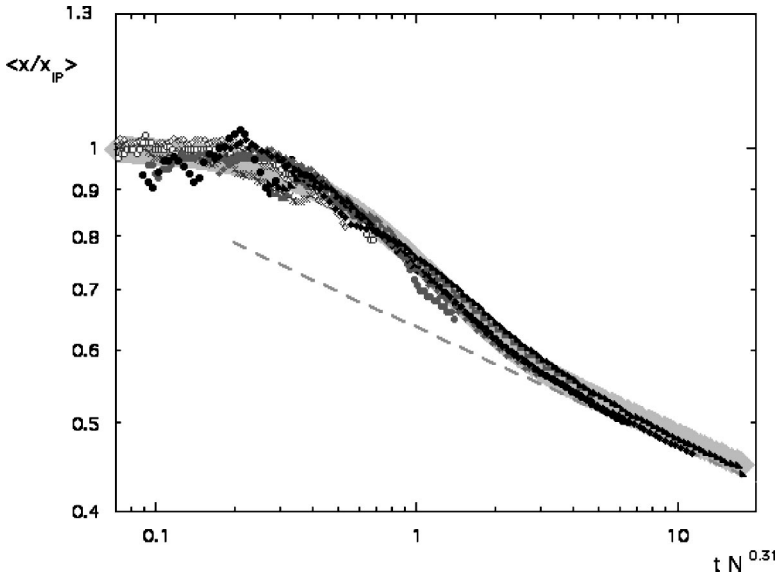

FIG. 4. The data for the average position of the injected fluid from Fig. 2 plotted vs the scaled time using the predictions in Eqs. (5) and (6). The plot symbols have the same meaning as in Figs. 2 and 3, i.e., the same legend is used. Apart from statistical noise the prediction leads to a credible collapse of the data. The dashed gray line represents the function $\langle x_{\mathrm{compact}}/x_{\mathrm{IP}}\rangle = \chi(t/\tau) = 0.637(t/\tau)^{-0.13}$. The heavy solid gray line, in the background, represents a fit to the scaling function, which will be discussed later; see Eq. (8).

in two dimensions, suggesting that it is likely valid in three dimensions.

Since the injected fluid advances linearly with time for compact flow, i.e., $x_{compact} \propto t$, for $t \gg \tau$, the scaling function in Eq. (6a) must vary with the -0.13 power of time for large t/τ; the dashed gray line in Fig. 4 shows this asymptotic behavior for the compact flow regime, $\langle x/x_{\mathrm{IP}}\rangle = \chi(t/\tau) \propto (t/\tau)^{-0.13}$. The extent to which the long time data for the average position has the same slope indicates that the average position is advancing linearly with time, thereby demonstrating the compact or linear behavior of the largest t/τ data.

Since the interfacial width becomes saturated (i.e., constant) for compact or stable flow, i.e., $w_{compact} \propto \mathrm{const}$, for $t \gg \tau$, the scaling function in Eq. (6b) must vary with the -1.13 power of time for large t/τ; the dashed gray line in Fig. 5 shows this asymptotic behavior for the compact flow regime, $\langle w/w_{\mathrm{IP}}\rangle = \Omega(t/\tau) \propto (t/\tau)^{-1.13}$. The extent to which the long time data has the same slope suggests that the interfacial width is crossing over from IPWT behavior to constant (i.e., stable) behavior.

This crossover in the average position was observed in our earlier paper [26]. However, at that time, we did not compare our results to the prediction of Wilkinson [1]. Furthermore, we had no results for the interfacial width, and the previously reported work was on smaller simulations, which had not achieved compact/linear/stable flow prior to breakthrough. To further demonstrate the compact/linear/stable behavior of the well-past-crossover flows, Figs. 6 and 7 show the data plotted so that the dashed-line behavior (of Figs. 4 and 5) is a constant. In Fig. 6, we present data for $t^{0.13}\langle x/x_{\mathrm{IP}}\rangle$ plotted vs t; since $x_{\mathrm{IP}} \approx 0.445 t^{1.13}$, this is essentially a plot of x/t. Before crossover, in the IPWT region this should increase with slope 0.13; well past crossover, this should be a constant. For the largest times and capillary numbers the data are constant. In Fig. 7, we present data for $w \approx 0.53(t/\tau)^{1.13}\langle w/w_{\mathrm{IP}}\rangle$ plotted vs t/τ; since $w_{\mathrm{IP}} \approx 0.53 t^{1.13}$, this is essentially a plot of w. Before crossover, in the IPWT region this should increase with slope 1.13; well past crossover, this should be a constant. For the largest times and

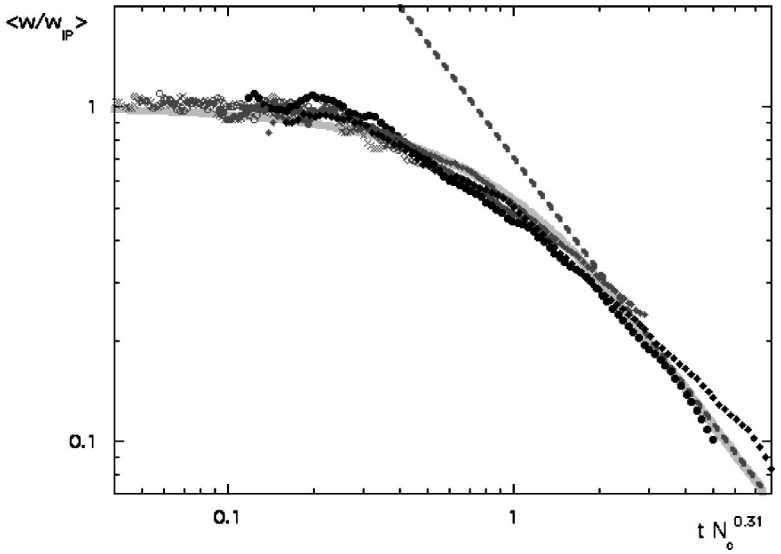

FIG. 5. The data for the interfacial width from Fig. 3 plotted vs the scaled time using the predictions in Eqs. (5) and (6). The plot symbols have the same meaning as in Figs. 2 and 3, i.e., the same legend is used. Apart from statistical noise, the collapse shows excellent agreement with the prediction of Wilkinson. The dashed line has slope -1.13. The heavy solid gray line, in the background, represents a fit to the scaling function, which will be discussed later; see Eq. (7).

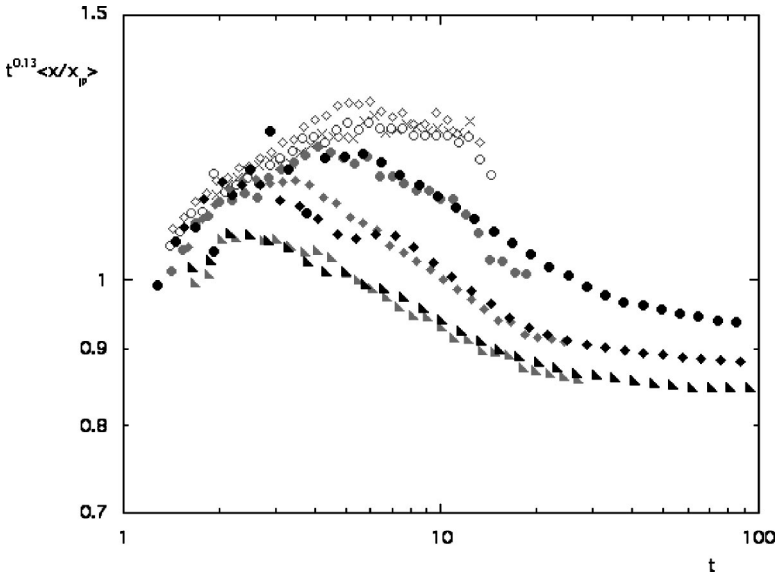

FIG. 6. The data from Fig. 2 plotted so that compact or linear behavior ($x_{compact} \propto t$) is constant on the figure (i.e., $t^{0.13}\langle x/x_{\mathrm{IP}}\rangle \propto x/t$). The plot only presents every third point to enhance the clarity of the legend.

capillary numbers, the data are essentially constant, but quite noisy.

Our two-dimensional pore-level modeling results for the average position of the injected fluid and the average interfacial width are entirely consistent with the crossover from the fractal flow characterized by invasion percolation with trapping to compact/linear/stable flow where the position of the interface (proportional to $\langle x\rangle$) advances linearly with time and where the width of the interface is constant. This crossover was first predicted by Wilkinson, who also predicted a characteristic length, Eq. (2), or equivalently a time, Eq. (5), for this crossover [1]. Our results are fully consistent with these predictions.

Having data for the form of the scaling functions, it is only natural for us to attempt to fit the data in Figs. 4 and 5 for the scaling functions $\chi(u)$ and $\Omega(u)$ in Eqs. (6a) and (6b). Since the interfacial width relaxes from the fractal behavior to a constant, the simple form

$$w = w_{\mathrm{IP}} \frac{\{1 - e^{-au^{1.13}}\}}{au^{1.13}} \tag{7}$$

is an appealing possibility, since it has the correct limiting behavior: $w = w_{\mathrm{IP}}\Omega(u) = w_{\mathrm{IP}}$ for small u, and $w \approx w_{\mathrm{IP}}\Omega(u) = w_{\mathrm{IP}}/au^{1.13} = \text{const}$ for large u. The heavy gray line in the background of Fig. 5 shows the best fit for this form of the scaling function $w/w_{\mathrm{IP}} = \Omega(u) = \{1 - e^{-au^{1.13}}\}/au^{1.13}$ using the one fitting parameter $a = 1.45 \pm 0.02$.

It is appealing to attempt to find a similar function for the scaling function, $\chi(u)$, associated with the average position. Here, we need a function which gives the constant behavior of $\chi(u)$ for small u, and the $u^{-0.13}$ dependence for large u. One rather complicated function was used in an earlier publication [26]; but it seems appealing to find a function similar to the simple one for the interfacial width in Eq. (7). One similar function with the correct limiting behaviors is

$$x = x_{\mathrm{IP}} \left\{ e^{-au^{1.13}} + \frac{(1 - e^{-au^{1.13}})}{bu^{0.13}} \right\}, \tag{8}$$

where $x = x_{\mathrm{IP}}\chi(u) = x_{\mathrm{IP}}$ for small u, and $x \approx x_{\mathrm{IP}}\chi(u) = x_{\mathrm{IP}}/bu^{0.13} \propto t$ for large u. The heavy gray line in the background of Fig. 4 shows the best fit of this simple approximation to the scaling function, $x/x_{\mathrm{IP}} = \chi(u) = e^{-au^{1.13}} + \{1 - e^{-au^{1.13}}\}/bu^{0.13}$, for values of the fitting constants $a = 1.26 \pm 0.02$ and $b = 1.533 \pm 0.006$. Although the simple functions in Eqs. (7) and (8) are only approximations to the true scaling functions, they do provide a reasonable prediction for

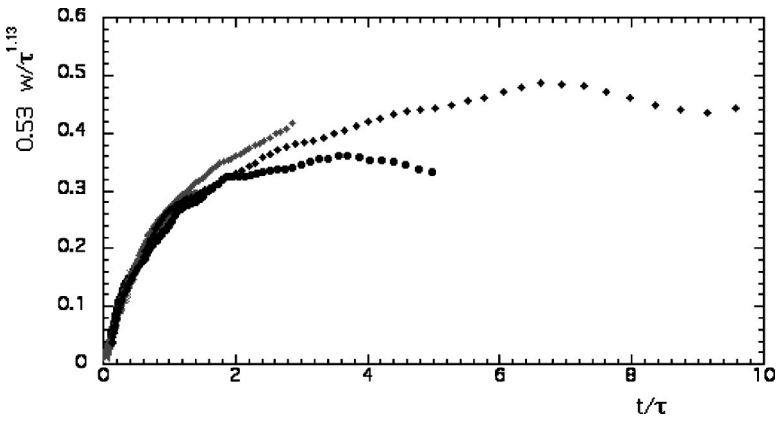

FIG. 7. The data from Fig. 5 plotted vs t/τ where $\tau = N_c^{-0.31}$ so that compact or stable behavior ($w_{compact} = \text{const}$) is constant on the figure $w \approx 0.53(t/\tau)^{1.13}\langle w/w_{\mathrm{IP}}\rangle$. Again, the long-time data for the width is noisier than that for the average position.

the scaling behavior of the interfacial width and the average position of the injected fluid.

III. CROSSOVER FROM CAPILLARY FINGERING TO COMPACT FLOW

A. Experimental flow patterns

In trying to compare our modeling results to experimental results in the literature, we confront several problems. For the small porous media studied in our modeling, we have definite predictions locating the crossover as a function of capillary number primarily from studying the average position of the injected fluid. Typical experimental results are near-breakthrough flow patterns for larger systems. These patterns show characteristic capillary fingering for small capillary numbers, while patterns at larger capillary numbers are compact. Qualitatively, this exhibits the change from IPWT to compact, stable, or linear; but it is hard to compare our modeling results with these experimental flow patterns for several reasons. First, because the experimental systems are usually larger, the inverse relationship between characteristic length and capillary number, Eq. (2), predicts that larger-scale breakthrough patterns, of length L, become compact at a much smaller capillary number, $N_c \approx L^{-1/0.38}$, than the smaller-scale breakthrough patterns from modeling. Secondly, our modeling results predict the capillary number dependence of the length scale related not to system size, L, but to average position of the injected fluid, $\langle x \rangle$. In the Appendix, we address these difficulties and attempt to locate the rather broad crossover regime for patterns of different length, L. From the results in the Appendix, we estimate that the crossover regime will begin with a capillary number [see Eq. (A4)], below which the flows will be IPWT fractals, and that the crossover regime will extend to a capillary number [see Eq. (A5)], above which the flows will be compact.

We can compare these predictions with flow patterns from two references [36,37]. In the first, the flow patterns in a two dimensional bead pack between two glass plates are shown in their Fig. 3 [37]. Given the size of their flow cell, the uniform diameter of the glass beads, and the porosity of the systems, which are all reported in the reference, we estimate the square flow cell has $L \times L = 378 \times 378$ beads. The patterns for the two smallest capillary numbers (and perhaps the next smallest) appear invasion percolation like, which is supported by their IPWT-like estimate of a fractal dimension for these three patterns. The patterns for the three largest capillary numbers appear compact. Taking $L = 378$, these equations locating the crossover predict that it should occur for capillary numbers between the lower and upper bounds in Eqs. (A4) and (A5) respectively, $2.8 \times 10^{-8} < N_c < 1.3 \times 10^{-6}$. The three obviously compact patterns have capillary numbers (3.38×10^{-5}, 2.14×10^{-5}, and 4.76×10^{-6}) greater than the predicted upper bound for the crossover regime. However, the IPWT-like patterns have capillary numbers (4.40×10^{-7}, 1.04×10^{-6}, and 2.12×10^{-6}) in the upper range of our predicted crossover regime, rather than the expected lower range. This suggests that the width of the crossover regime may be influenced by other factors: e.g., the much larger porosity in the experiments (70% versus the 32% in the model) or differences between experiment and the model in the amount and kind of randomness, etc. However, the simple scaling arguments given in the Appendix do allow estimates for locating the crossover, which are approximately correct.

The flow patterns in Fig. 4 of the other reference show patterns at three different times for each of five capillary numbers in an etched glass flow cell, which is 10.4 cm in the direction of flow [36]. The etched glass plates have a diamond-lattice array (as in our model) of pore throats, which are 0.1365 cm long. The distance, in the flow direction, between adjacent rows of throats is $0.1365 \text{ cm}/\sqrt{2}$, so that there are $10.4/(0.1365 \text{ cm}/\sqrt{2}) = 107$ rows of throats along the flow direction from inlet to outlet. Instead of the left-hand set of patterns, which shows the flow shortly after injection, or the right-hand set, which shows the patterns well past breakthrough, let us consider the middle set of patterns in Fig. 4, which show the flow when the injected fluid is about three-quarters of the way through the porous medium [36]. For this middle set, the maximum extent of the injected fluid is approximately three fourths of the full 107 rows (or somewhat less), so that $L \approx 80$. Taking $L = 80$, the equations locating the crossover predict that it should occur for capillary numbers between the lower and upper bounds in Eqs. (A4) and (A5), respectively, $1.7 \times 10^{-6} < N_c < 7.6 \times 10^{-5}$. In this case, our equations slightly overestimate the capillary numbers at which crossover occurs. However, these experiments were performed for a very favorable viscosity ratio where the viscosity of the nonwetting, injected fluid was much more viscous than the defending, wetting fluid, specifically $M = \mu_{nw}/\mu_w = 26$. In a recent paper, we estimated that, for favorable viscosity ratios, the characteristic crossover time should be approximately $\tau \approx (M^{0.39} N_c)^{0.31}$ [42]. Dividing Eqs. (A4) and (A5) by the factor of $M^{0.39}$, our upper or lower bound estimates become $4.7 \times 10^{-7} < N_c < 2 \times 10^{-5}$ with the midpoint being $N_c^m = 3 \times 10^6$. Their most IPWT-like pattern [their Fig. 4(e)] has a capillary number $N_c = 6.5 \times 10^{-7}$ which is a bit larger than our estimate of the initiation of crossover [36]. Their Fig. 4(c) appears transitional and has a capillary number, $N_c = 1.3 \times 10^{-6}$ which is near the predicted midpoint. Their Fig. 4(b) appears compact and has a capillary number, $N_c = 6.5 \times 10^{-6}$, which is halfway between our estimate of the midpoint and the upper bound. Again, our estimates of the bounds on the crossover regime, given by Eqs. (A4) and (A5) produce reasonable estimates locating the crossover region, though the experimental crossover regions seem narrower than those from modeling.

B. Quantitative reanalysis of experimental results

In addition to the qualitative observation of the crossover from the flow patterns in Fig. 3 of Ref. [37], this paper also presented quantitative analyses, which can be compared with our modeling results and with the earlier predictions of Ref. [1]. This reference argues that the interfacial width should have the form

$$w = t^{\beta_d} h(t/w_s^{1/\beta_d}),$$

where β_d is the dynamic exponent and w_s is the saturated front width, i.e., the width at long times or equivalently the

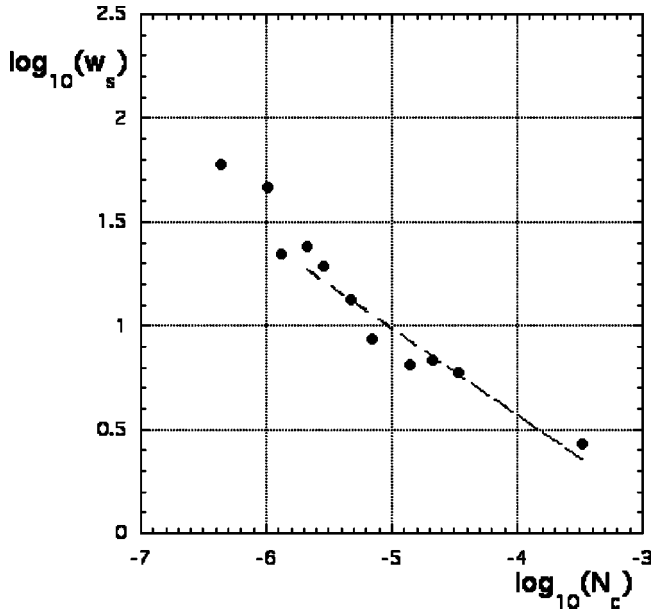

FIG. 8. The data from Ref. [37] for the log of the "saturated" front width vs the log of the capillary number, N_C (denoted Ca in Ref. [37]). Excluding the three points with the smallest capillary numbers, a linear fit predicts a slope -0.42 ± 0.05 which is consistent with the prediction of -0.38 by Wilkinson [1]. A recent paper has similar results for w_s from pore level modeling [43].

characteristic length scale given in Eq. (2). Basically, this is equivalent to our Eq. (6b). Our modeling results from our pore level model and from our analysis of IPWT simulations indicate that β_d is simply related to the fractal dimension so that $\beta_d = 1/(D_f - 1)$ which has values in the range 1.13 for our small systems up to 1.2 for large systems. The authors state that it was "difficult to get a very precise value" for the dynamic exponent; they estimate $\beta_d = 0.8 \pm 0.3$, the upper limit of which is near the postulated value of 1.13 to 1.2 [38]. For long times, the scaling form becomes

$$w = t^{\beta_d} h(t/w_s^{1/\beta_d}) \approx w_s.$$

Wilkinson predicted that this saturated front width should have a power law dependence upon capillary number $w_s = \Lambda \approx N_c^{-\nu/(t+1-\beta+\nu)}$, where the indices are the usual indices from critical percolation theory. As we have seen, in two dimensions this exponent has the value 0.38, which agrees with our modeling results for both the average position of the injected fluid and the interfacial width. From the analysis of their experiments, Frette *et al.* estimate that this exponent is 0.6 ± 0.2. However, as they state "it is possible that the slowest experiment has not reached saturation." Since we know that the flow crosses over from IPWT behavior, where $w \approx t^{1/(D_f-1)}$ and then crosses over to compact behavior (i.e., saturates) for $t \gg w_s^{1/\beta_d} \approx N_C^{-0.31}$, the width will not have achieved its saturated value until the flow is compact. Since their box-counting for the three slowest experiments indicate a fractal dimension consistent with IPWT, these three slowest experiments do not exhibit compact flow and cannot have achieved a saturated front width. Figure 8 shows the data presented in the paper (their Table 1 and plotted in their Fig. 4) for width vs capillary number [37]. Figure 8 also shows a fit to all but the three smallest capillary numbers; this fit yields a value, 0.42 ± 0.05, consistent with Wilkinson's prediction of 0.38.

IV. CONCLUSIONS

We have presented results from pore-level modeling in two dimensions for the average position of the injected fluid (related to the position of the interface) as well as the width of the interface between the injected, nonwetting fluid and the defending, wetting fluid. These results are entirely consistent with the predicted crossover from the fractal flow characterized by invasion percolation with trapping (IPWT) to compact/linear/stable flow where the position of the injected fluid advances linearly with time and where the width of the interface is constant.

Wilkinson's prediction for the characteristic length scale, Eq. (2), accounts for all the capillary number dependence of the average position and interfacial width, i.e., $\langle x(t) \rangle$ and $\langle w(t) \rangle$ are well represented by scaling functions of scaled time, Eqs. (6a) and (6b) [1]. Our results allow fits to the scaling functions which provide closed form expressions for the dependence of average position and interfacial width upon capillary number and time. A reinterpretation of experimental results from the literature agrees with the predictions of Wilkinson and our pore-level modeling [37]. It should be noted that Wilkinson used general flow and percolation theory arguments, which are "universal" in that they are independent of a particular porous media structure, in both two and three dimensions. The validity of his general derivation is supported by the agreement of his predictions with results from our simplistic, diamond-lattice porous media structure. Although many aspects of the flow are different in two and three dimensions, e.g., values of fractal dimensions and other exponents and the topology of the flow, our results provide evidence supporting the validity of his derivation of Eq. (2) for any standard porous media structure in two and three dimensions.

The size scaling inherent in the crossover predictions enable us to predict the location of the crossover, i.e., values of capillary numbers which bracket the crossover regime, for two-dimensional systems of different sizes. These predictions were compared with flow patterns from flow cell experiments in the literature [36,37]. These comparisons indicate that the experiments exhibit the crossover in approximately the same range of capillary numbers predicted by our modeling.

ACKNOWLEDGMENT

M.F. acknowledges the support of the U. S. Department of Energy, Office of Fossil Energy.

APPENDIX: LOCATING THE CROSSOVER FOR PATTERNS OF DIFFERENT LENGTH

Here we address the roadblocks in our attempt to locate the rather broad crossover regime in systems of different

size. Because of the inverse relationship between characteristic length and capillary number, Eq. (2), experimental breakthrough patterns for larger systems, of length L, become compact at a much smaller capillary number, $N_c \propto L^{-1/0.38}$, than the smaller-scale breakthrough patterns from our modeling. Secondly, our modeling results predict the capillary number dependence of the length scale related not to system size, L, but to average position of the injected fluid, $\langle x \rangle$. We will use our modeling results in an attempt to estimate the capillary numbers at which near breakthrough flow patterns of length L have (i) just initiated crossover, at N_c^I and (ii) have fully crossed over to compact flow, at N_c^C.

First let us review our modeling results to characterize the crossover region as observed in Figs. 2, 4, and 6. In Figs. 2 and 4, it is possible to determine a crude estimate of the capillary number at which crossover begins for our $L=30$ systems near breakthrough, i.e., crossover has just begun for the smallest capillary number $N_c=1.33\times10^{-5}$. Therefore, for a system of length L, scaling would predict that near breakthrough flows should have begun to crossover for a capillary number [labeled (I,1) to denote the initiation of crossover for this first method], $N_C^{(I,1)}=1.33\times10^{-5}\ (30/L)^{1/0.38}$.

On the other hand, the crossover to compact or linear flow is nearly completed for our $L=30$ systems at the next-to-largest capillary number $N_c=8.85\times10^{-4}$, so that the flow should be compact for a capillary number [labeled (C,1) for compact], $N_C^{(C,1)}=8.85\times10^{-4}\ (30/L)^{1/0.38}$. These first estimates are somewhat crude, especially for the start of crossover, $N_c^{(I,1)}$ because from Figs. 2, 4, and 6, it is clear that crossover initiated well before breakthrough for the smallest capillary numbers shown.

Since we have characterized the crossover in terms using the average position of the injected fluid as a function of time (actually the volume of injected fluid divided by the width of the medium), it seems natural to use these results provided that we can relate the average position of the injected fluid in the pattern, $\langle x \rangle$ to pattern length, i.e., the maximum extent of the injected fluid, $L=x_{\max}$. For pistonlike flow, the injected fluid fully floods the medium out to $L=x_{\max}$ so that, at breakthrough, the average position of the injected fluid is one-half this distance $\langle x \rangle = L/2$.

We can determine the relationship between $\langle x \rangle$ and L for IPWT from the behavior of the saturation profile. In an earlier reference, we argued that the saturation profile should obey the simple scaling relation

$$S(x,t) = t^{-0.13}\Sigma(x/t^{1.13}), \tag{A1}$$

where the $S(x,t)\ dx$ gives the fraction of porous medium occupied by the injected fluid within dx of x at time t [44]. This scaling form for the saturation profile was verified for million site IPWT systems for a range of times up to breakthrough, as shown in Fig. 9. The fit to the scaling function in Fig. 9 is given by

$$\Sigma(u) = 0.695\exp(-0.172u) + 0.275\exp(-2.54u). \tag{A2}$$

If we estimate the value of the maximum of injected fluid, $x_{\max}$, to occur where $\Sigma(u_m)=0.01$ then $x_{\max}=u_m t^{1.13}$, where

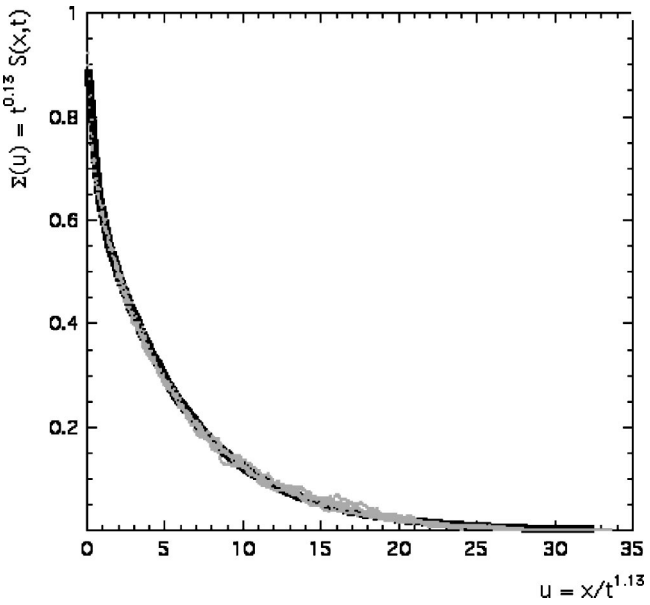

FIG. 9. Scaling of saturation profile for IPWT on million site porous media for a range of times up to breakthrough [44]. The heavy black line shows the simple fit to the data used to estimate the relationship between $\langle x \rangle$ and $x_{\max}$.

$u_m=24.65$; note this underestimates the value of $x_{\max}$ since the fluid will have extended beyond this 1% limit. Since the average position of the injected fluid is simply the first moment of this saturation profile divided by its zeroth moment, we can use Eqs. (A1) and (A2) to determine the average position at any time. We find $\langle x \rangle = 5.67t^{1.13}$. At breakthrough, this predicts

$$\frac{L}{\langle x \rangle} \geqslant 4.35. \tag{A3}$$

The greater than or equal to symbol is used because $\Sigma(u_m)=0.01$ uses a slight underestimate of $x_{\max}$.

Therefore, for IPWT the length of a porous medium should be greater than or equal to approximately four times the average position of the injected fluid at breakthrough.

In addition, data for the average position of the injected fluid at breakthrough from IPWT simulations for systems with a variety of lengths corroborate the above result that $\langle x \rangle \approx L/4$. Of course, this is only valid for IPWT; for more compact cases it will be closer to $\langle x \rangle \approx L/2$.

Using our results (Figs. 2, 4, and 6) from characterizing the crossover in the average position, $\langle x \rangle$, one can locate the crossover regime as a function $\langle x \rangle$, and capillary number, N_c. Using the above relationship between average position, $\langle x \rangle$, and maximum extent, L, will allow a determination of the crossover regime in terms of maximum extent and capillary number. Figure 10 demarcates the region of crossover. Up to the first diamond the flows are described by IPWT, while after the last diamond the flows are compact with the average position and interface advancing linearly with time. The location of these points allows a determination of the values of $\langle x \rangle$ and t in terms of capillary number as follows.

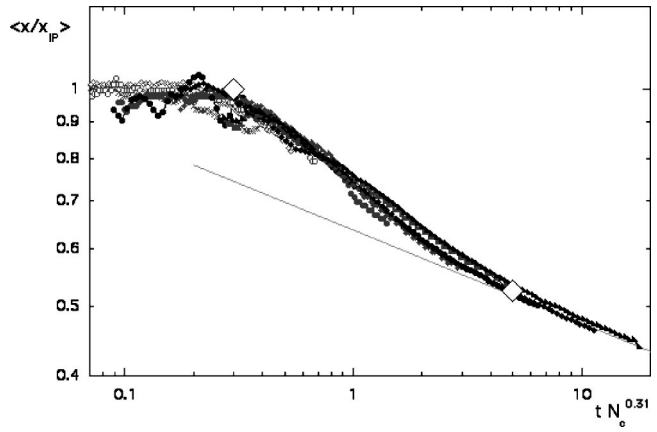

FIG. 10. Demarcation of the limits of the crossover: (i) the initiation of crossover at the end of the IPWT regime at the first diamond and (ii) the end of crossover at the second diamond, after which the flows are compact advancing linearly with time.

(i) The initiation of crossover at the end of the IPWT regime occurs at $t=0.3/N_c^{0.31}$ and at $\langle x\rangle=0.115/N_c^{0.38}$, i.e., for capillary number $N_c=(0.115/\langle x\rangle)^{1/0.38}$ so that, in terms of L, $N_c\approx(0.115\times4.4/L)^{1/0.38}=2.2\times10^{-5}(30/L)^{1/0.38}$; this should be compared with our earlier result $N_c^{(I,1)}=1.33\times10^{-5}(30/L)^{1/0.38}$, which was likely an underestimate.

(ii) The end of crossover, where the flows are compact advancing linearly with time, occurs at $t=5/N_c^{0.31}$ and at $\langle x\rangle=1.52/N_c^{0.38}$, i.e., for capillary number $N_c=(1.52/\langle x\rangle)^{1/0.38}$; so that, in terms of L (for compact flow $\langle x\rangle=L/2$) at breakthrough, compact flow occurs for capillary numbers greater than $N_c^{(C,2)}\approx(1.52\times2/L)^{1/0.38}=2.4\times10^{-3}(30/L)^{1/0.38}$. This should be compared with our earlier result, $N_c^{(C,1)}=8.85\times10^{-4}(30/L)^{1/0.38}$. Combining the two, we estimate $N_c^{C}=1\times10^{-3}(30/L)^{1/0.38}$.

The values of average position were determined using the result $\langle x_{IP}\rangle=0.445t^{1.13}$ [45].

Summarizing these results, we estimate that the flow should be described by IPWT for capillary numbers less than

$$N_c^{I}\approx2.2\times10^{-5}(30/L)^{1/0.38}, \tag{A4}$$

and that the flow will be compact for capillary numbers greater than

$$N_c^{C}\approx1\times10^{-3}(30/L)^{1/0.38}. \tag{A5}$$

Therefore, we estimate that systems of maximum extent L will be in the crossover regime for capillary numbers between the estimates in Eqs. (A4) and (A5)

$$N_c^{I}<N_c<N_c^{C}. \tag{A6}$$

[1] D. Wilkinson, Phys. Rev. A **34**, 1380 (1986).
[2] R. J. Blackwell, J. R. Rayne, and W. M. Terry, Trans. AIME **216**, 1 (1959).
[3] R. E. Collins, *Flow of Fluids through Porous Materials* (Reinhold, New York, 1961).
[4] J. Bear, *Hydraulics of Ground Water* (McGraw-Hill, New York, 1979).
[5] F. A. L. Dullien, *Porous Media: Fluid Transport and Pore Structure* (Academic, New York, 1979).
[6] H.-K. Rhee, R. Aris, and N. R. Amundson, *First-Order Partial Differential Equations: Vol. I (Theory and Applications of Single Equations)* (Prentice Hall, Englewood Cliffs, NJ, 1986).
[7] R. Lenormand, E. Touboul, and C. Zarcone, J. Fluid Mech. **189**, 165 (1988).
[8] M. Blunt and P. King, Phys. Rev. A **42**, 4780 (1990).
[9] M. Sahimi, *Flow & Transport in Porous Media & Fractured Rock From Classical Models to Modern Approaches* (VCH Verlagsgesellschaft, Germany, 1994).
[10] J. Feder, *Fractals* (Plenum, New York, 1988).
[11] T. Vicsek, *Fractal Growth Phenomena* (World Scientific, Singapore, 1989).
[12] M. Ferer *et al.*, Phys. Rev. A **45**, R6973 (1992).
[13] M. Ferer and D. H. Smith, Phys. Rev. E **49**, 4114 (1994).
[14] M. Ferer, *et al.*, AIChE J. **49**, 749 (1995).
[15] M. Ferer, J. Gump, and D. H. Smith, Phys. Rev. E **53**, 2502 (1996).
[16] P. Meakin, *Fractals, Scaling, and Growth Far From Equilibrium* (Cambridge University Press, Cambridge, England, 1998).
[17] R. Chandler *et al.*, J. Fluid Mech. **119**, 249 (1982).
[18] D. Wilkinson and J. F. Willemsen, J. Phys. A **16**, 3365 (1983).
[19] M. J. Blunt, Curr. Opin. Colloid Interface Sci. **6**, 197 (2001).
[20] D. Wilkinson, Phys. Fluids **28**, 1015 (1984).
[21] N. Martys, M. Cieplak, and M. Robbins, Phys. Rev. Lett. **66**, 1058 (1991).
[22] M. O. Robbins *et al.*, Phys. Rev. Lett. **71**, 2074 (1993).
[23] D. Wilkinson, Phys. Rev. A **30**, 520 (1984).
[24] J. F. Gouyet, M. Rosso, and B. Sapoval, Phys. Rev. B **37**, 1832 (1988).
[25] M. Ferer, G. S. Bromhal, and D. H. Smith, Physica A **319**, 11 (2003).
[26] M. Ferer, G. S. Brohmal, and D. H. Smith, Phys. Rev. E **67**, 051601 (2003).
[27] M. Sahimi, H. T. Davis, and L. E. Scriven, Chem. Eng. Commun. **23**, 329 (1983).
[28] M. Sahimi and A. O. Imdakm, J. Phys. A **21**, 3833 (1988).
[29] J.-D. Chen and D. Wilkinson, Phys. Rev. Lett. **55**, 1892 (1985).
[30] S. C. van der Marck, T. Matsuura, and J. Glas, Phys. Rev. E **56**, 5675 (1997).
[31] E. Aker, "A Simulation for Two-Phase Flow in Porous Media," thesis, University of Oslo, 1996.
[32] E. Aker *et al.*, Transp. Porous Media **32**, 163 (1998).
[33] E. Aker, K. Jorgen-Maloy, and A. Hansen, Phys. Rev. E **58**, 2217 (1998).
[34] E. Aker, K. Jorgen-Maloy, and A. Hansen, Phys. Rev. E **61**, 2936 (2000).
[35] G. Pereira, Phys. Rev. E **59**, 4229 (1999).

[36] C. D. Tsakiroglou, M. A. Theodoropoulou, and V. Karoutsos, AIChE J. **49**, 2472 (2003).
[37] O. I. Frette *et al.*, Phys. Rev. E **55**, 2969 (1997).
[38] M. Ferer, G. S. Brohmal, and D. H. Smith, Physica A **334**, 22 (2004).
[39] In Ref. [13], we argued that the interfacial width could be determined from the first $\langle x \rangle$ and second $\langle x^2 \rangle$ moments of the saturation profile; specifically that the width w was given by $w^2 = 2(3\langle x^2 \rangle - 4\langle x \rangle^2 + \langle x \rangle)$.
[40] A. P. Sheppard *et al.*, J. Phys. A **323**, L521 (1999).
[41] M. Ferer *et al.*, Phys. Rev. E **47**, 2713 (1993).
[42] M. Ferer, G. S. Brohmal, and D. H. Smith, *Computational Methods in Water Resources*, edited by Cass T. Miller, M. W. Farthing, W. G. Gray, and G. F. Pindar (Elsevier, Amsterdam, 2004), p. 153.
[43] C. D. Tsakiroglou, J. Non-Newtonian Fluid Mech. **117**, 1 (2004).
[44] M. Ferer, G. S. Bromhal, and D. H. Smith, Physica A **311**, 5 (2002).
[45] In our powers of capillary number we use the correct, large system limit of fractal dimension; hence the 1.21 power instead of the 1.13 power used in characterizing our small scale modeling.